ISSN: 2688-8645

Design of UHF RFID Tag Antenna for Metallic Surfaces

Shijie Miao, Peng Wang *, Zhenhua Liu, Qiaohong Hao, Weiyi Qu

[1] Hebei University of Water Resources and Electric Engineering, Cangzhou Hebei, 061001, China

[2] Hebei Industrial Manipulator Control and Reliability Technology Innovation Center, Cangzhou, Hebei, China

* Corresponding author: Peng Wang (Email: wangpengzgsd@163.com)

Abstract

To address the challenges of information exchange and enable real-time status monitoring of components awaiting remanufacturing, this paper presents a semi-flexible UHF RFID tag antenna designed for direct mounting on metallic objects. Numerical simulations were conducted to analyze the transmission coefficient and mutual impedance patterns, achieving conjugate impedance matching between the antenna and the chip, thereby establishing the desired resonant frequency. The antenna's resonant frequency can be conveniently adjusted via coarse and fine tuning of specific geometric parameters. Experimental validation, conducted according to a predefined protocol, measured the antenna's resonant frequency in both free-space and on-metal environments. The results demonstrate maximum read ranges of 11.5 m on a metal-free surface and 6.2 m on an aluminum alloy steel pipe, with the resonant frequency consistently maintained within the 860 MHz to 960 MHz range. The proposed antenna exhibits robust anti-metal characteristics, making it highly suitable for application on large metallic surfaces commonly found in remanufactured products.

Keywords

UHF RFID; Antenna; Conjugate Matching; Resonant Frequency; Anti-metal Property.

1. Introduction

The General Office of the State Council has issued the "Opinions on Accelerating the Establishment of a Waste Recycling System," which explicitly calls for "promoting the remanufacturing of end-of-life equipment" and "exploring new pathways for waste recycling." This initiative is of significant importance for safeguarding national resource security, advancing carbon peak and carbon neutrality goals steadily, and fostering a green transformation of the development model. Remanufacturing, defined as an industrial process that restores end-of-life products to a like-new condition, is distinguished by its potential for energy and material conservation as well as environmental protection [1,2]. By maximizing the value retained in waste resources [3], it has emerged as a key enabler of the circular economy. Key technologies in this field encompass disassembly, cleaning, inspection, remaining life assessment, processing and forming, assembly, and quality evaluation [4]. However, logistics and inventory management across these interconnected stages often suffer from a lack of product information, leading to increased processing time and labor costs. Furthermore, monitoring the in-service status of remanufactured products is essential. Consequently, a critical challenge in the remanufacturing process is the effective management of information flow between these technical stages to enable real-time status acquisition of components awaiting repair and to oversee operational conditions throughout the process.

ISSN: 2688-8645

Current automatic identification technologies primarily include barcode recognition, biometrics, optical character recognition (OCR), integrated circuit (IC) cards, and radio frequency identification (RFID) [5-7]. Among these, RFID technology has been widely adopted in the manufacturing and logistics sectors due to its advantages of low cost, passive operation, wireless capability, and extended read range. RFID systems operate by detecting changes in inductive coupling or variations in backscattered signals, with Ultra-High Frequency (UHF) RFID specifically relying on the backscatter principle. However, when UHF RFID technology is deployed in metallic environments, the radiation efficiency of the tag antenna is significantly degraded. This degradation results in resonant frequency detuning, reduced gain, and distortion of the antenna's radiation pattern.

In recent years, considerable research has focused on the development of anti-metal RFID tag antennas. Based on their feeding and radiation mechanisms, these antennas are generally classified into three categories: dipole antennas, microstrip patch antennas, and planar inverted-F antennas (PIFAs). When a dipole antenna is placed directly on a metal surface, its induced current is effectively canceled by the mirrored current generated within the metal [8], rendering the antenna inoperable. In contrast, conventional microstrip patch antennas consist of a patterned radiating patch and a dielectric substrate, which separates the structure into a ground plane and an antenna layer. Within the ground plane, induced currents are predominantly confined to the surface adjacent to the dielectric substrate. This configuration minimizes interaction with the underlying metal surface, thereby providing the tag with inherent anti-metal interference capabilities [9–11]. Planar inverted-F antennas are also well-suited for metallic structures; their size can be reduced by incorporating vias or short-circuiting walls, facilitating compliance with deployment constraints. In wireless communication systems, both microstrip patch and planar inverted-F antennas are widely regarded as low-cost, compact solutions. Their integrated ground plane effectively isolates the radiating element from the mounting surface, significantly mitigating adverse interactions with metal [12,13].

The UHF RFID tag antenna proposed in this paper is specifically designed for deployment on large metallic surfaces, offering both long read range and a degree of mechanical flexibility. This characteristic renders it suitable for application on curved metal objects, thereby addressing the challenge of identifying metallic items in logistics and related industries. The remainder of this paper is structured as follows. Section 2 analyzes the antenna's anti-metal properties and the underlying theory of impedance matching. Section 3 presents the antenna design and dimensional optimization using simulation software. Section 4 describes the experimental setup and provides a comprehensive analysis and discussion of the measurement results. Finally, Section 5 concludes the paper.

2. Impedance Matching Theory

Impedance matching between the tag antenna and the chip is a critical factor in radio frequency identification (RFID) systems, as it directly governs key transmission performance metrics, including maximum read range, transmission power, backscattered power, and radar cross-section. The chip's impedance is modulated by controlling the connection state of an internal parallel capacitor [14]. When the capacitor is disconnected, the chip presents a load state with an impedance denoted as Z_{C1}; when the capacitor is connected, the load state transitions to Z_{C2}. To elucidate the impedance modulation mechanism, the antenna and chip can be equivalently represented using a Thevenin circuit, as illustrated in Figure 1. Here, $Z_{antenna} = R_a + jX_a$ denotes the complex impedance of the antenna, and $Z_{chip} = R_c + jX_c$ represents the complex impedance of the chip (load). As the chip switches between load states, the impedance matching condition varies, thereby modulating the amplitude of the backscattered signal. This amplitude modulation enables the wireless transmission of sensing data. In an ideal matched condition,

ISSN: 2688-8645

where the antenna impedance is the complex conjugate of the chip impedance, the transmission power required to activate the chip is minimized. It is important to note that the chip behaves as a nonlinear load; its complex impedance in each state is dependent on both frequency and input power. Furthermore, the chip's power consumption determines its activation threshold (minimum voltage or power) and the corresponding impedance value [15].

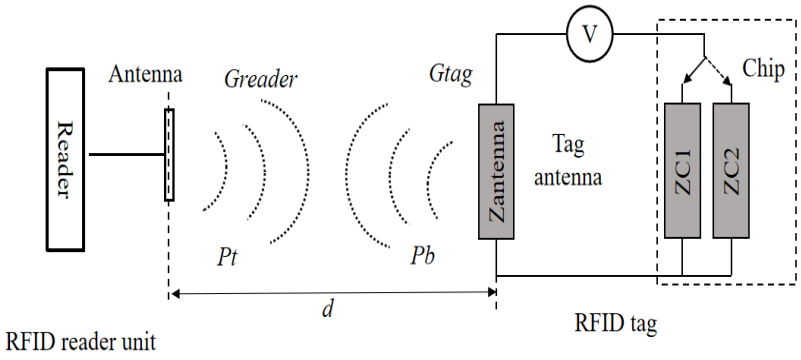

Fig 1. Schematic diagram of impedance modulation

3. Structural Design and Size Optimization of the Tag Antenna

A typical microstrip tag antenna consists of three layers: a top radiating patch, an intermediate dielectric substrate, and a bottom ground plane. The RFID chip is electrically connected to the radiating patch using soldering or conductive adhesive. Once the target operating frequency is established, the length of the patch antenna can be calculated, while its width is generally constrained to be less than the length. Consequently, impedance matching for the tag sensor is primarily achieved by adjusting the geometry(specifically the dimensions or shape) of the internal structure of the radiating patch [16].

The proposed tag antenna incorporates an electrically small loop into the main radiating patch via asymmetric connecting lines. This configuration enables impedance tuning by adjusting the loop's perimeter and the relative positions of the connecting lines. The patch antenna is fabricated on a bilayer substrate consisting of a 50-μm-thick polyimide (PI) layer (εr=3.5, tanδ=0.08) on top of a 3-mm-thick foam layer (εr=1.12). This bilayer design not only provides the desired mechanical flexibility but also mitigates the adverse effects of metallic surfaces on antenna performance, with the foam layer additionally offering structural support. The radiating patch and ground plane are made from 15-μm-thick copper foil, bonded to the upper and lower surfaces of the composite substrate. Based on the selected Alien Higgs-3 chip [17], calculations using Equations (1) and (2) yield a chip impedance of 29.6−j208.6 Ω at the 880 MHz frequency band. The tag antenna was subsequently designed following the step-by-step procedure outlined below.

Step 1: Determining the dimensions of the radiating patch

According to the cavity model theory for microstrip antennas, the radiating patch, along with the dielectric substrate and ground plane, forms a resonant cavity. The resonant frequency of this cavity is primarily determined by the physical length of the patch. Specifically, the electrical length L_e of the patch is slightly greater than its physical length L_1 , while the substrate thickness h is much smaller than the operating wavelength. Optimal radiation performance is achieved when the electrical length L_e is slightly less than half the guided wavelength (λ/2) within the dielectric substrate. Under this condition, the physical length L_1 of the radiating patch can be estimated using the following formula:

$$L_1=0.49\lambda_d=0.49\frac{\lambda}{\sqrt{\varepsilon_r}}=0.49\frac{c}{f\sqrt{\varepsilon_r}} \quad (1)$$

ISSN: 2688-8645

where λ_d is the wavelength in the dielectric substrate, ε_r is its relative permittivity of the dielectric substrate, λ is the free-space wavelength, c is the speed of light in free space, and f is the tag's operating frequency.

The dielectric substrate selected for the proposed tag antenna is polyimide (PI), which has a relative permittivity of ε_r=3.5 at room temperature. Substituting this value into the above formula yields an estimated patch length of

$$L_1=\frac{0.49\times3\times10^8\text{m/s}}{880\times106\times\sqrt{3.5}\text{Hz}}=0.089\text{m}=89\text{mm} \quad (2)$$

The proposed antenna adopts a microstrip structure with an electrically small loop serving as the feeding element. Impedance tuning is achieved by adjusting the loop's perimeter, its embedding depth within the patch, and the relative position of the asymmetric connecting lines. The overall dimensions of the tag antenna are 90 mm × 70 mm × 3.13 mm, comprising a 50-μm-thick PI layer and a 3-mm-thick foam layer. This configuration ensures a wide bandwidth while providing good mechanical flexibility to the tag. A 2 mm × 4 mm area is reserved on the patch for chip mounting. With the overall dimensions fixed, the geometry of the radiating patch and the specific dimensions of its internal structures were optimized using the finite element method (FEM) solver, HFSS.

Step 2: Tag antenna simulation and optimization

To determine the internal structural dimensions and achieve the desired impedance for the radiating patch antenna, electromagnetic simulations were conducted using HFSS, a finite element method (FEM) solver. The simulation model was constructed by defining the antenna geometry, assigning appropriate boundary conditions, and generating the mesh. Material properties were assigned based on the software's built-in library, with polyimide (PI) and foam specified for the dielectric substrates. The RFID chip was modeled as a lumped port with an impedance of 29.6−j208.6 Ω, positioned between the tuning stub and the radiating patch. The radiating patch, tuning stub, and ground plane were all modeled as perfect electric conductors (PEC). An air domain of dimensions 300mm×300mm×300mm was defined and assigned a radiation boundary condition. Adaptive meshing was then performed. To ensure convergence and accuracy, the solution was configured with a center frequency of 880 MHz, a maximum of 11 iterative passes, and a maximum convergence error of 0.02. A fast frequency sweep was conducted over a linear frequency range from 860 MHz to 960 MHz with a step size of 1 MHz.

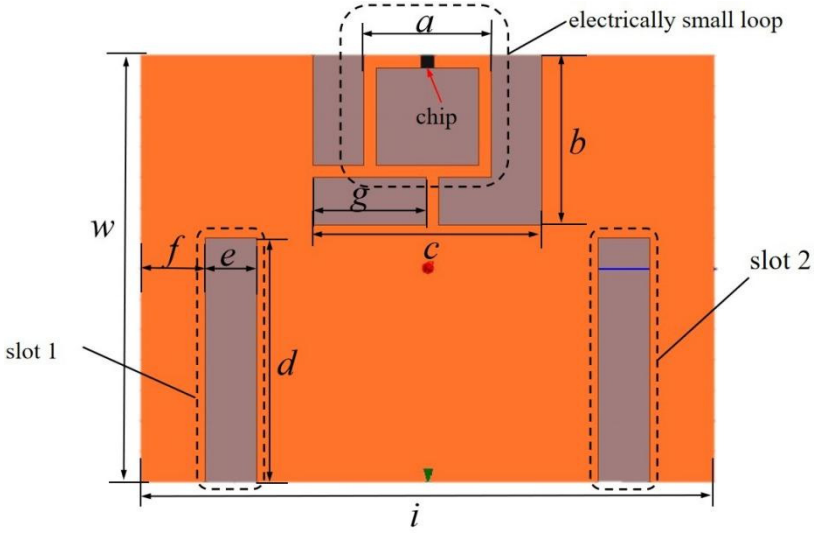

Fig 2. The geometry of tag

ISSN: 2688-8645

Figure 2 illustrates the geometry of the proposed tag antenna. As shown, the antenna's structure is defined by several key parameters: the square side length (*a*), the middle notch width (*c*), the slot length (*d*), the slot width (*e*), and the bottom segment length (*g*). The overall dimensions of the antenna are denoted by length (*l*) and width (*w*). Parameters *a*, *c*, *d*, *e*, and *g* serve as optimization variables for tuning the antenna's performance. To achieve the desired impedance matching, these geometric parameters were optimized using HFSS. Based on the target resonant frequency, an objective function was constructed within the software's Optimetrics module, and a genetic algorithm with a unity weighting coefficient was employed for the optimization process. Parametric studies were conducted to investigate the influence of (*a*), (*c*), (*d*), (*e*), and (*g*) on the input impedance and reflection coefficient (S11) of the antenna. Figure 3 presents the simulated effect of varying the parameter *a* on the antenna's resistance and reactance. As observed in Figure 3(a), increasing *a* causes a gradual decrease in the resonant frequency, with the reflection coefficient remaining below -30 dB throughout the simulated range. This behavior is attributed to the corresponding increase in both the resistive and reactive components of the antenna's input impedance with larger *a*, effectively shifting their values and resulting in a downward shift of the resonant frequency, as confirmed in Figure 3(b).

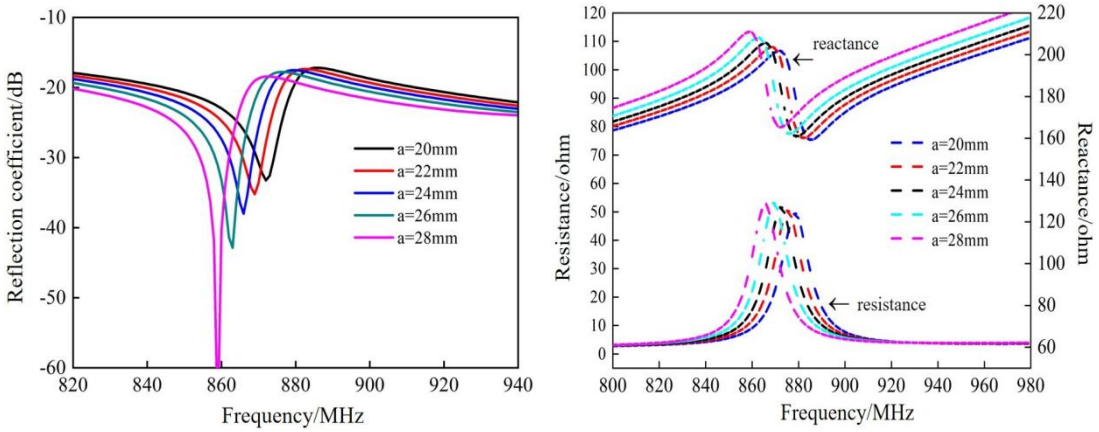

(a) reflection coefficient (b) input impedance

Fig 3. Effect of variation in dimension *a* on reflection coefficient and input impedance

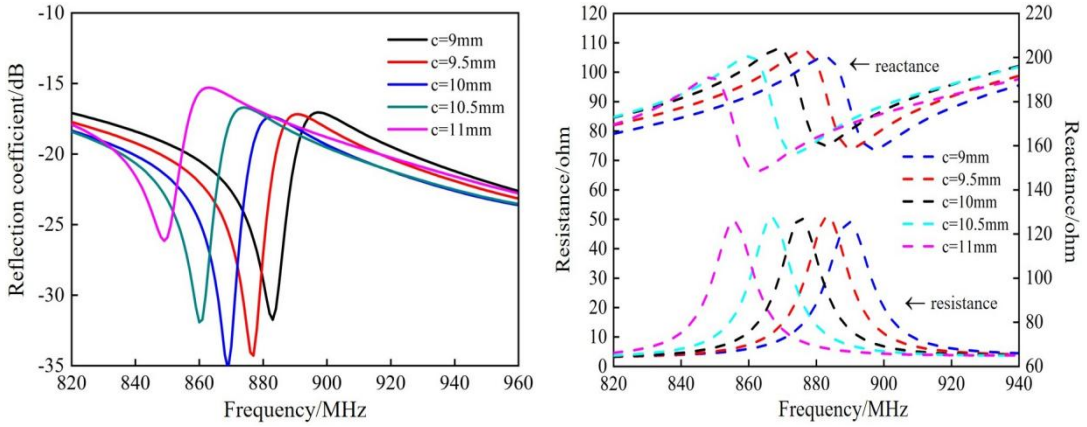

(a) reflection coefficient (b) input impedance

Fig 4. Effect of variation in dimension *c* on reflection coefficient and input impedance

Figure 4 illustrates the effect of varying the parameter c on the input impedance and reflection coefficient (S11). As shown in Figure 4(a), increasing *c* causes a pronounced leftward shift (toward lower frequencies) of the resonant frequency. This behavior is primarily attributed to

ISSN: 2688-8645

the significant influence of parameter *c* on both the real and imaginary parts of the antenna's input impedance, as depicted in Figure 4(b). Similarly, increasing the slot length (*d*) leads to the most substantial shift in resonant frequency among all parameters examined. As shown in Figures 5(a) and 5(b), this increase results in a higher reflection coefficient (S11) and a leftward shift in both the resistive and reactive components of the impedance. Consequently, coarse tuning of the tag antenna's resonant frequency—that is, rapidly adjusting it to the target UHF band—can be achieved by modifying the square side length (*a*), the middle notch width (*c*), and the slot length (*d*).

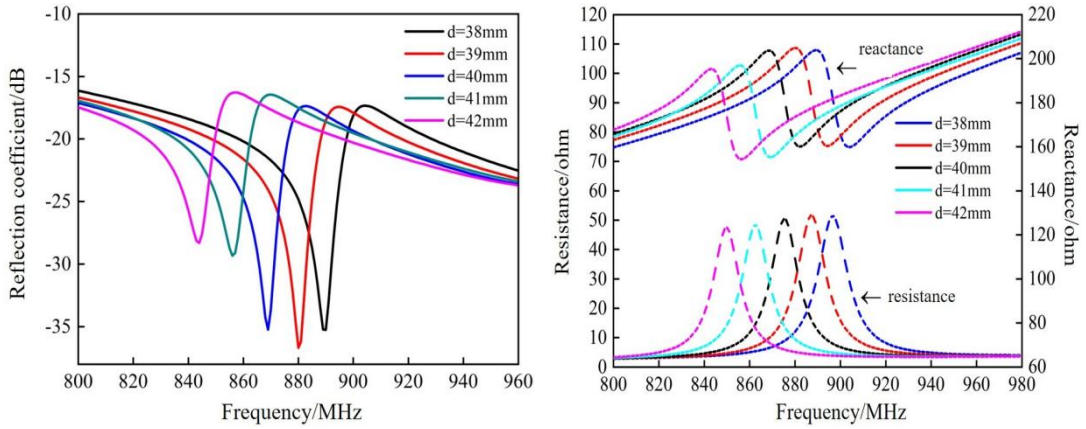

(a) reflection coefficient (b) input impedance

Fig 5. Effect of variation in dimension *d* on reflection coefficient and input impedance

Table 1 summarizes the sensitivity of each design parameter to the tag's resonant frequency. During the design process, parameters with a sensitivity greater than 10 MHz/mm are initially used to coarsely tune the resonant frequency into the target UHF band. Subsequently, parameters with a sensitivity below 10 MHz/mm are utilized for fine-tuning to achieve the precise desired frequency.

Following simulation and optimization, the optimal geometric parameters for the proposed antenna were determined, as summarized in Table 2. The optimized dimensions are as follows: square side length *a*=22 mm, middle notch width *c*=10 mm, slot length *d*=41 mm, slot width *e*=8.4 mm, and bottom segment length *g*=16 mm, with all other parameters remaining unchanged. Based on these dimensions, the final tag antenna model was established.

Table 1. Tuning sensitivity of design parameters

parameter	adjust sensitivity (MHz/mm)	parameter	adjust sensitivity (MHz/mm)
a	15	*d*	11.5
c	15.5	*e*	9
g	0.5		

Table 2. Optimized parameter dimensions of the tag antenna structure

parameter	*a*	*c*	*d*	*e*	*g*
size/mm	22	10	41	8.4	16

Figure 6 presents the simulated power transmission coefficient (τ) and the three-dimensional gain pattern of the proposed antenna. As shown in Figure 6(a), at the resonant frequency of 883 MHz, τ reaches 0.87, indicating satisfactory impedance matching between the antenna and the chip, and consequently, good power transmission efficiency. Figure 6(b) shows that the

ISSN: 2688-8645

antenna achieves its maximum gain (highlighted in red) along the *x*- and *z*-axes, further confirming its favorable radiation performance.

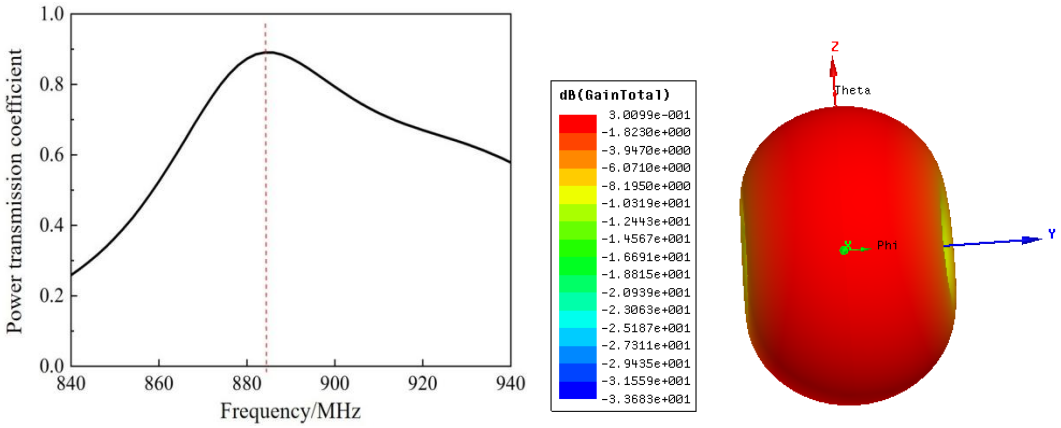

(a) power transmission coefficient (b) three-dimensional gain

Fig 6. Power transmission coefficient and 3D gain

4. Results and Discussion

The resonant frequency and read range of the proposed tag antenna were measured using the Tagformance Pro measurement system (Voyantic, Finland) [18], as illustrated in Figure 7. The measurement system operates in compliance with the ISO 18000-6C protocol, ensuring compatibility with standard RFID readers. The Tagformance Lite reader was paired with a linearly polarized patch antenna, matching the polarization of the UHF tag antenna under test. Frequency sweeps were performed over the 860-960 MHz UHF band with step sizes of 0.5 MHz and 1 MHz. Power sweeps were conducted with step sizes of 0.1 dBm and 0.5 dBm. After configuring the parameters, the system automatically executed the frequency and power sweeps. Throughout the measurements, the communication distance between the reader antenna and the tag antenna was kept constant. The system was controlled, and measurement data were retrieved via a USB 3.0 interface. To eliminate environmental and path-dependent effects, the system was calibrated using a reference tag prior to testing, ensuring the reliability of the measurement results.

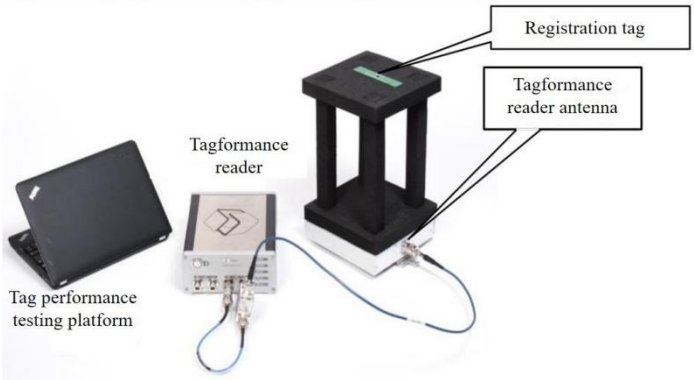

Fig 7. Tagformance Pro performance test system

The tag antenna prototype was fabricated by bonding the Higgs-3 chip to the designated pads on the antenna using conductive adhesive, a process carried out by an external partner, as shown in Figure 8(a). For performance evaluation, the tag was tested under two conditions: mounted on the surface of an aluminum alloy steel pipe (diameter: 20 cm) and placed on a metal-free surface supported by a black foam stand, as illustrated in Figure 8(b). Following system calibration and setup, the tag's read range and resonant frequency were measured.

ISSN: 2688-8645

Figure 9 presents the simulated and measured read ranges. When the tag was placed on the foam support (a metal-free environment), the simulated read range was 12 m with a resonant frequency of 890 MHz, while the measured values were 11.5 m and 885 MHz, respectively. The slight discrepancy of 0.5 m between simulation and measurement was primarily attributed to fabrication tolerances and the presence of the conductive adhesive layer, which were not accounted for in the simulation model. When the tag was attached to the curved surface of the aluminum alloy steel pipe, the simulated read range was 7.9 m with a resonant frequency of 880 MHz, while the measured read range was 6.2 m at 869 MHz. The reduced read range on the metallic pipe, compared to the metal-free case, is primarily due to the bending of the tag, which decreases its effective radiation area and consequently reduces the backscattered power received by the reader.

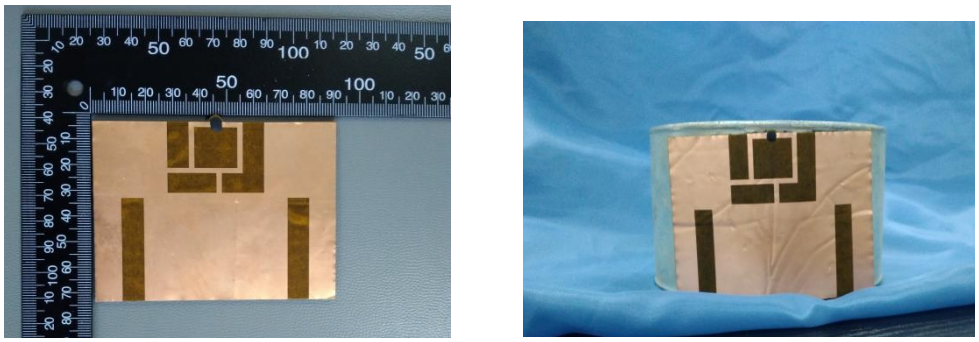

(a) the fabricated tag antenna (b) mounted on a curved metal surface

Fig 8. Prototype of the tag antenna

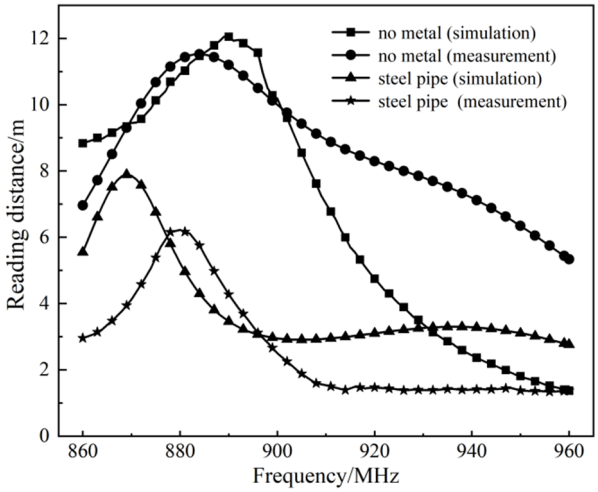

Fig 9. Reading distance of the tag antenna

5. Conclusion

The proximity of the metal surface introduces parasitic capacitance to the tag antenna, detuning the impedance matching between the chip and the radiating patch and thereby degrading overall transmission performance. Incorporating a dedicated ground plane effectively isolates the antenna from these parasitic effects, endowing the proposed design with inherent anti-metal properties.

This paper proposes a semi-flexible UHF RFID tag antenna designed for direct mounting on metallic surfaces. The antenna achieves effective impedance tuning through inductive coupling between its feeding loop and two integrated slots, enabling both coarse and fine frequency adjustments via geometric optimization. Experimental results demonstrate maximum read

ISSN: 2688-8645

ranges of 11.5 m in free space and 6.2 m when mounted on an aluminum alloy steel pipe, with resonant frequencies consistently within the 860-960 MHz UHF RFID band. The proposed design exhibits robust anti-metal properties, making it a promising candidate for integration onto the large metallic surfaces typical of remanufactured products. Future work will focus on further enhancing its anti-metal performance and miniaturizing the antenna footprint to accommodate a broader range of remanufactured components.

6. Summary

The paper proposes a semi-flexible UHF RFID tag antenna designed for metallic surfaces, which achieves conjugate impedance matching and resonant frequency adjustability through geometric optimization. Experimental results indicate maximum read ranges of 11.5 m on metal-free surfaces and 6.2 m on aluminum alloy steel pipes, with resonant frequencies maintained within the 860-960 MHz band, demonstrating its robust anti-metal performance suitable for remanufactured product applications.

Acknowledgments

This work was supported by the Hebei Provincial Training Program of Innovation and Entrepreneurship for Undergraduates (No. S202410085052), and Self-funded Projects under the Cangzhou City Key Research and Development Program (No. 23244101033), and the Fundamental Research Funds for the Hebei University of Water Resources and Electric Engineering (No. SYKY2411).

References

[1] B. S. Xu. Theory and technology of equipment remanufacturing engineering [M]. National Defense Industry Press, 2007.

[2] S. Xu, S. Y. Dong, and P. J. Shi. Current status and prospects of quality assurance technology systems for remanufactured parts with Chinese characteristics[J]. Journal of Mechanical Engineering, Vol. 20 (2013) No. 49, p. 84-90.

[3] V. Daniel R and Guide Jr. Production planning and control for remanufacturing: industry practice and research needs[J]. Journal of Operations Management, Vol. 18 (2000) No. 4, p. 467-483.

[4] S. Zhu and J. K. Yao. Remanufacturing technology and processes [M]. China Machine Press, 2011.

[5] X. F. Wu and D. C. Chen. Radio frequency identification technology[M]. Publishing House of Electronics Industry, 2006.

[6] Z. W. Zhang. Theory and practice of radio frequency identification technology[M]. China Science and Technology Press, 2008.

[7] Q. Zeng, O. Y. Ouyang, and T. Wang. Radio frequency identification and electronic tags. Beijing, China: China Economic Publishing House, 2005.

[8] T. Tang, C. Liao, and G. H. Du. Design of a miniaturized UHF folded dipole anti-metal RFID tag antenna[J]. Journal of Microwaves, Vol. 4 (2012) No. 28.

[9] H. D. Chen, Y. H. Tao and C. Y. Kuo. Low-profile radio frequency identification tag antenna using a trapezoid patch mountable on metallic surfaces[J]. Microwave & Optical Technology Letters, Vol. 52 (2010) No. 8, p. 1697-1700.

[10] B. Yu, S. J. Kim, B. Jung, et al. RFID tag antenna using two-shorted microstrip patches mountable on metallic objects[J]. Microwave & Optical Technology Letters, Vol. 49 (2010) No. 2, p. 414-416.

[11] S. L. Chen and K. H. Lin. A slim RFID tag antenna design for metallic object applications[J]. IEEE Antennas & Wireless Propagation Letters, Vol. 7 (2009) p. 729-732.

[12] G. Shi, Y. He, B. Yin, et al. Analysis of mutual couple effect of UHF RFID antenna for the internet of things environment[J]. IEEE Access, Vol. 7 (2019) p. 81451-81465.

ISSN: 2688-8645

[13] Y. G. He, P. L. She, L. Zuo, et al. Frequency offset study in mutual coupling effects of UHF RFID near-field systems [J]. Journal of Electronics & Information Technology, Vol. 41 (2019) No. 3, p. 670–678.

[14] S. Caizzone, and G. Marrocco. RFID-Grids for deformation sensing[C]. IEEE International Conference on RFID (RFID), Orlando, 2012.

[15] R. Li, G. Dejean, M. M. Tentzeris, et al. FDTD analysis of patch antennas on high dielectric-constant substrates surrounded by a soft-and-hard surface[J]. Magnetics IEEE Transactions on, Vol. 40 (2004) No. 2, p. 1444-1447.

[16] J. Zhang and Y. Long. A miniaturized via-patch loaded dual-layer RFID tag antenna for metallic object applications[J]. IEEE Antennas& Wireless Propagation Letters, Vol. 12 (2013) No. 8, p. 1184-1187.

[17] Alien (2016), Higgs-3 EPC class 1 gen 2 RFID tag IC, available at https:// www.alientechnology.com.

[18] Tagformance [online]. voyanitic tagformance pro, available at: http://voyantic.com/products.